# Angular Broadening of Intraday Variable AGN. II. Interstellar and Intergalactic Scattering

T. Joseph W. Lazio
Naval Research Laboratory, 4555 Overlook Ave. SW, Washington, DC 20375-5351; USA
Joseph.Lazio@nrl.navy.mil

## Roopesh Ojha

NVI/United States Naval Observatory, 3450 Massachusetts Ave. NW, Washington DC 20392-5420; USA rojha@usno.navy.mil

## Alan L. Fey

United States Naval Observatory, 3450 Massachusetts Ave. NW, Washington DC 20392-5420; USA afey@usno.navy.mil

## Lucyna Kedziora-Chudczer

Institute of Astronomy, School of Physics A28, The University of Sydney, NSW 2006; Australia

## James M. Cordes

Department of Astronomy, Cornell University and NAIC, Ithaca, NY 14853; USA cordes@astro.cornell.edu

and

David L. Jauncey and James E. J. Lovell

Australia Telescope National Facility CSIRO, PO Box 76, Epping, NSW 1710; Australia

### ABSTRACT

We analyze a sample of 58 multi-wavelength, Very Long Baseline Array observations of active galactic nuclei (AGN) to determine their scattering properties. Approximately 75% of the sample consists of AGN that exhibit centimeter-wavelength intraday variability (interstellar scintillation) while the other 25% do not show intraday variability. We find that interstellar scattering is measurable for most of these AGN, and the typical broadening diameter is 2 mas at 1 GHz. We find that the scintillating AGN are typically at lower Galactic latitudes than the non-scintillating AGN, consistent with the scenario that intraday variability is a propagation effect from the Galactic interstellar medium. The magnitude of the inferred interstellar broadening measured toward the scintillating AGN, when scaled to higher frequencies, is comparable to the diameters inferred from analyses of the light curves for the more well-known intraday variable sources. However, we find no difference in the amount of scattering measured toward the scintillating versus non-scintillating AGN. A consistent picture is one in which the scintillation results from localized regions ("clumps") distributed throughout the Galactic disk, but which individually make little contribution to the angular broadening. Of the 58 AGN observed, 37 (64%) have measured redshifts. At best, a marginal trend is found for scintillating (non-scintillating) AGN to have smaller (larger) angular diameters at higher redshifts. We also use our observations to try to constrain the possibility of intergalactic scattering. While broadly consistent with the scenario of a highly turbulent intergalactic medium, our observations do not place significant constraints on its properties.

#### 1. Introduction

There is now compelling evidence that the intraday variability (IDV) phenomenon—intensity variations on hour time scales at centimeter wavelengths in compact, flat-spectrum, extragalactic sources (e.g., Heeschen 1984; Quirrenbach et al. 1992)—is of extrinsic origin. Density fluctuations in the interstellar medium (ISM) induce refractive index fluctuations which, when combined with the relative motions of the scattering medium and the Earth, produce intensity variations or scintillations. The evidence for this conclusion is both differences in the variability pattern arrival times at widely spaced radio telescopes and annual cycles in the variability characteristics for various IDV sources (Jauncey et al. 2000; Jauncey & Macquart 2001; Rickett et al. 2001; Dennett-Thorpe & de Bruyn 2002; Dennett-Thorpe & de Bruyn 2003; Jauncey et al. 2003, 2006; Bignall et al. 2006).

In order to exhibit interstellar scintillations (ISS), a source must contain a sufficiently compact component (analogous to "Stars twinkle, planets don't") such that its angular diameter is comparable with or smaller than the size of the first Fresnel zone of the scattering screen, i.e., of order tens of microarcseconds at frequencies near a few gigahertz (e.g., Walker 1998). The absence of ISS in a source could be either an intrinsic or extrinsic effect. Active galactic nuclei (AGN) might have a range of intrinsic diameters, in which case only the most compact would exhibit ISS. Alternately, interstellar density fluctuations produce a rich range of observable phenomena (Rickett 1990), of which scintillations are only one manifestation. Angular broadening along the line of sight, due either to multiple ionized media or an extended medium, could produce apparent diameters of AGN sufficiently large that the AGN would not display ISS.

Consistent with this requirement for a compact ( $\sim 10~\mu as$ ) component, Ojha et al. (2004) have compared AGN that display ISS with those that do not and find that the scintillating AGN typically are more core-dominated on a milliarcsecond scale than the non-scintillating AGN. This result is striking given that their observations compared the source structure on milliarcsecond, not microarcsecond, scales. However, the observations of Ojha et al. (2004) were at the single frequency

of 8.4 GHz. This frequency is sufficiently high that interstellar scattering effects on most lines of sight through the ISM would not be detectable on terrestrial baselines nor could they have exploited the wavelength dependence for scattering to separate the its effects from the intrinsic diameters of the sources.

The AGN observed by Ojha et al. (2004) were drawn from the Micro-Arcsecond Scintillation-Induced Variability (MASIV) survey (Lovell et al. 2003). The MASIV survey is a large variability survey of the northern sky with the primary goal being the construction of a large sample of scintillating AGN. The survey used the Very Large Array (VLA) at 5 GHz in a multi-array mode and has yielded scintillation information on over 500 AGN, of which over half have been found to be scintillating (Lovell et al. 2007).

Ojha et al. (2006) presented multi-frequency observations of a subset of MASIV sources. Their observations were designed to create a sample of sufficient size to compare and contrast the scattering behavior of scintillating and non-scintillating AGN. This paper reports the analysis of those observations.

#### 2. Source Sample

Our sample consists of 58 AGN, observed in two different programs. The first subset consists of 49 AGN from the MASIV survey, observed over 3 days with the Very Long Baseline Array (VLBA) in 2003 February. At the time of the observations, approximately half of these 49 AGN were classified as highly variable MASIV sources, with scintillation indices larger than 2%; the other half were classified as non-scintillators, with no scintillation index larger than 0.2%. These sources were chosen without regard to their Galactic latitude or longitude. Since our observations, however, further MASIV observations and analysis shows that many of the AGN identified originally as non-scintillating are in fact scintillating (Lovell et al. 2007). The number of recognized scintillating AGN is now 46, and the number of non-scintillating sources is now 13 (ratio of 3:1). The subset of AGN from the MASIV survey were observed at 0.33, 0.61, and 1.6 GHz, with additional observations at 2.3 and 8.4 GHz. In total, 194 VLBA images of the 49 MASIV extragalactic radio sources at up to 7 observing frequencies were obtained (Ojha et al. 2006). Additional data were obtained from the United States Naval Observatory (USNO) Radio Reference Frame Image Database<sup>1</sup> (RRFID) and the literature.

The observations of these 49 AGN were acquired by cycling through the sources so as to increase the u-v plane coverage. Typical times on source range from 10 min. at the higher frequencies to 25 min. at the lower frequencies. Typical noise levels were within a factor of 2–3 of the expected thermal noise limits.

Ojha et al. (2006) fit gaussian component models to the visibility data of the sources, using the images as guides. If more than one component was required to model a source at a given frequency, the most compact component was identified as the "core," as the most compact component will be the one for which scattering effects will be most apparent. The most compact component is frequently the brightest one. For the few sources where this does not hold strictly at all frequencies, the compact and bright component that could consistently be identified as the same at all frequencies was identified as the "core," e.g., J0713+4349 where the northernmost component is identified as the core even though it is not the brightest component at 8.4 GHz (Ojha et al. 2006).

The second subset consists of 9 AGN chosen from those used to define the International Celestial Reference Frame (Johnston et al. 1995; Ma et al. 1998). The initial motivation was to use these AGN to search for scattering resulting from the interstellar media of galaxies along their lines of sight. The sources were chosen to be (1) At Galactic latitudes  $|b| > 45^{\circ}$ ; (2) Strong, with  $S_{6\,\mathrm{cm}} \approx 1$  Jy; and (3) Compact and dominated by a single component (Fey & Charlot 1997). Observations of these 9 sources were conducted with the VLBA on 2001 February 17 and 18 at 0.33 and 0.61 GHz. Calibration, imaging, and model extraction was performed in a manner similar to that used by Ojha et al. (2006).

Because both subsets involved observations at 0.33 and 0.61 GHz, the observations were generally carried out at night so that the sources had large solar elongations. Indeed, observing at large solar elongation was an explicit criterion in

scheduling the observations for the second subset. As a result, the smallest elongation for any source is  $75^{\circ}$ , and the typical elongation is approximately  $130^{\circ}$ .

For the present analysis, we have used the core components models from these two observing programs, augmented by measurements from the literature. All sources have angular diameters measured at at least 3 frequencies, and some sources have measured angular diameters at as many as 7 frequencies. See Table 2 of Ojha et al. (2006). While the selection criteria for the two subsets differed, the sources were treated identically in the following analysis.

#### 3. Analysis

Angular broadening is manifested as an observed angular diameter that scales approximately as  $\lambda^2$ . We fit the measured angular diameters to the functional form

$$\theta^2 = (\theta_s \nu^{-2.2})^2 + (\theta_i \nu^x)^2 \tag{1}$$

where  $\theta_s$  and  $\theta_i$  are the scattering and intrinsic (FWHM) diameters of the AGN, respectively, at the fiducial frequency of 1 GHz. We found the best-fitting values for  $\theta_s$  and  $\theta_i$  in a minimum  $\chi^2$  sense. We considered both x=0 (i.e., frequency-independent intrinsic diameter, for a flat spectrum source) and x=-1 (i.e., frequency scaling for a single incoherent synchrotron component) and selected the value of x that produced the lower  $\chi^2$ .

As a motivation for the use of equation (1), as well as anticipating later discussion, we begin by considering a crude approximation to equation (1). For the sources having measured angular diameters at both 0.33 and 1.6 GHz, we have assumed a simple power-law scaling for the angular diameter,  $\theta \propto \nu^{\beta}$ , and solved for  $\beta$ . We chose 0.33 GHz because the frequency dependence of scattering means that it will be the most sensitive to scattering; we chose 1.6 GHz as the second frequency as an attempt to balance between having a sufficiently large frequency dynamic range so as to obtain a robust estimate of  $\beta$  but not having such a large frequency range that intrinsic structure might dominate. If scattering is important, we expect  $\beta \approx -2$ . We find an average value of  $\bar{\beta} = -1.9 \pm 0.1$  for the entire sample. Clearly, we

<sup>1</sup> http://www.usno.navy.mil/RRFID/

anticipate that intrinsic structure may be important for some sources, but that the  $\bar{\beta}$  is close to the expected value from scattering indicates that scattering is important for the sample of sources as a whole.

Table 1 summarizes the inferred scattering and intrinsic diameters from fitting the data for each source to equation (1). For comparison, we also list the predicted diameter at 1 GHz from the NE2001 model (Cordes & Lazio 2006) for interstellar scattering,  $\theta_{\rm NE2001}$ . Figure 1 illustrates examples of the measured angular diameters, showing the results for an AGN for which a relatively large amount of scattering is inferred and one for which a relatively small amount of scattering is inferred.

Table 1
Fitted Scattering and Intrinsic Diameters

J0102+5824 124.419 -4.435 0.644 Y 1 3.6 1.2 6 6 J0217+7349 128.927 11.964 2.367 N 1 2.8 0.5 9 11	4.9 2.0 1.9 4.1 1.5
J0217+7349 128.927 11.964 2.367 N 1 2.8 0.5 9 11	2.0 1.9 4.1 1.5
	4.1 1.5
J0343+3622 $157.530$ $-14.691$ $1.484$ Y 1 $3.2$ $3.7$ 5 $39$	4.1 1.5
$J_{0349+4609}$ $J_{52.152}$ $J_{6.369}$	1.5
$J0403+2600$ $168.025$ $-19.648$ $2.109$ $Y_1$ $0$ $2.4$ $0.3$ $8$ $17$	3.8
**************************************	3.8
$J0419+3955$ $160.461$ $-7.336$ $\cdots$ $Y$ $0$ $2.6$ $0.2$ $3$ $2$	
J0423+4150 159.705 -5.381 2.277 Y 0 4.1 0.5 3 0.3	4.6
J0451+5935 $149.323$ $9.660$ ··· Y 0 $4.9$ 0.2 3 8	2.9
$J0502+1338$ $187.414$ $-16.745$ $\cdots$ Y 0 3.7 0.1 3 1	1.6
J0503+0203 $197.911$ $-22.815$ N 0 4.6 0.5 8 10	1.2
$J0507+4645$ $161.025$ $3.716$ $\cdots$ $Y_1$ $0$ $1.6$ $1.0$ $3$ $9$	5.2
$J0509+0541$ $195.405$ $-19.635$ $\cdots$ $Y$ $0$ $3.0$ $0.2$ $5$ $24$	1.3
$10539 + 1433^{a}$ $191.597$ $-8.660$ $2.69$ Y $1$ $3.4$ $2.4$ $3$ $3$	3.1
J0539+1433 <sup>a</sup> 191.597 -8.660 2.69 Y 0 6.1 0.4 3 3	3.1
30535+1435 $131.337$ $-8.000$ $2.03$ $1$ $0$ $0.1$ $0.4$ $3$ $3$ $3$ $3$ $3$ $3$ $3$ $3$ $3$ $3$	1.3
J0007+0720 140.804 20.838 1.97 1 <sub>1</sub> 0 1.4 0.4 11 20	1.5
J0650+6001 155.842 23.155 0.455 Y 0 7.8 0.3 6 36	1.3
$J0654+5042$ $165.680$ $21.106$ $\cdots$ $Y_1$ $0$ $1.8$ $0.2$ $3$ $45$	1.4
J0713+4349 173.792 22.199 0.518 N 1 1.3 4.7 11 18	1.4
$J0721+7120$ 143.981 28.017 2.06 $Y_1$ 1 0.6 0.9 8 39	1.1
J0725+1425 203.643 13.908 ··· Y 0 1.5 0.2 6 36	1.7
$J0738+1742$ 201.846 18.070 0.424 $Y_1$ 0 1.4 0.2 9 38	1 5
	1.5
$J0745+1011$ 209.796 16.592 2.624 $Y_1$ 1 0.6 2.2 10 36	1.4
J0757+0956 211.311 19.057 0.266 Y 0 1.1 0.2 9 24	1.3
$J0808+4950$ $169.163$ $32.564$ $1.418$ $Y_1$ $1$ $1.1$ $1.1$ $12$ $35$	1.1
J0830+2410 200.021 31.876 0.939 Y 1 0.8 1.9 6 9	1.2
$J0831+0429$ 220.693 24.331 0.180 $Y_1$ 1 4.8 1.0 9 18	1.1
$J0842+1835  207.275  32.480  1.270 \qquad Y_1 \qquad 0  4.1 \qquad 0.5  8  23$	1.1
J0914+0245 228.352 32.819 0.427 Y 0 2.8 0.1 4 16	1.0
J0920+4441 175.700 44.815 2.190 N 1 1.7 0.7 10 36	1.0
J0956+2515 205.511 50.981 0.712 Y 1 0.0 2.3 11 31	0.9
700K0 / MOV	0.6
J0958+4725 170.055 50.730 1.882 Y 0 2.3 0.2 7 7	0.9
J1008+0621 233.521 46.012 ··· Y 0 5.0 0.0 3 8	0.9
J1014+2301 210.699 54.431 0.565 Y 0 3.5 0.3 7 37	0.9
J1041+5233 $157.521$ $54.965$ $0.677$ Y $0$ $1.4$ $0.8$ 4 $1$	0.8
$J1125+2610$ $210.920$ $70.885$ $2.341$ $Y_1$ $1$ $0.6$ $1.1$ $5$ $18$	0.6
$J1153+8058$ $125.719$ $35.836$ $1.250$ $Y_1$ $0$ $1.9$ $0.2$ $6$ $17$	0.9
J1159+2914 199.413 78.374 0.729 Y 1 2.7 1.5 8 18	0.5

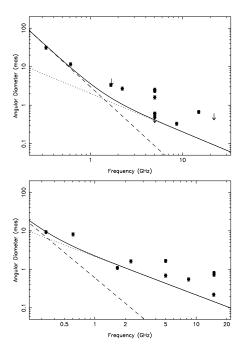


Fig. 1.— Two examples of fitting results. For both plots, solid circles show measured diameters, arrows indicate upper limits, the solid line indicates the fit of equation (1) to the observations, the dashed line indicates the inferred scattering diameter, and dotted line indicates the inferred intrinsic diameter. Uncertainties on the angular diameters are plotted, but in many cases are comparable to the size of the symbol. *Top* The source J2022+6136 for which a relatively large scattering diameter, 3.1 mas at 1 GHz, is inferred. *Bottom* The source J0745+1011 for which a relatively small scattering diameter, 0.6 mas at 1 GHz, is inferred.

There are values of the reduced  $\chi^2$  in Table 1 that are larger than unity, at times by a significant factor. These result from a combination of two factors. First, the uncertainties for some data are likely to be underestimated. For the observed diameters obtained from our observations, we estimated their uncertainties using a bootstrap-like procedure in which visibility data associated with different antennas were removed before performing the fit. The range of fitted diameters suggests a 10% uncertainty. For angular diameters obtained from the literature, we have assumed the same fractional uncertainty. However, we have been able to identify data for which this assumed

10% is likely to be too small.

The fitting procedure also yields an estimate of the uncertainty in the inferred scattering diameter (at 1 GHz). The median value of this uncertainty is 0.1 mas. We have repeated the fitting procedure with larger uncertainties adopted for the angular diameters obtained from the literature, and in some cases even removing apparent outliers. The typical change in the inferred diameter is comparable to the uncertainty in the inferred scattering diameter. We have also repeated analyses described below with larger uncertainties for the angular diameters from the literature and find no change from the results we present below.

A second potential cause of large  $\chi^2$  values is that we have adopted fixed frequency scaling exponents in equation (1). We might obtain a better fit by letting x be a fitted parameter, fitting the scattering frequency dependence rather than adopting -2.2, or both. To do so would often require more data than are available. Consequently, while larger than unity, we consider there to be plausible explanations for the  $\chi^2$  values in Table 1 and shall use the angular diameters resulting from our fits.

Oiha et al. (2006) divided the sources into two groups, "scintillators" and "non-scintillators." Since the publication of that paper, it has been realized that some of the AGN identified as scintillators displayed variation at only a single epoch ("once-er") among the MASIV observations, leading to the possibility that a non-scintillator would be classified mistakenly as a scintillator. Analysis of the MASIV observations (to be published elsewhere) suggests that the light curve from an individual epoch can be classified correctly at the 95% confidence level. From the four epochs of observations comprising MASIV, the probability of a false identification is only 4.3\%, meaning that we expect only 1 source in our sample to be classified mistakenly. While we identify the singleepoch variable sources in Table 1, their presence should have have no significant effect on our analysis, and we treat the single-epoch variable AGN as scintillators. Also, analysis has continued on the MASIV sources, so there may be occasional differences in the classification (scintillating vs. non-scintillating) in our Table 1 as compared to Table 1 of Oiha et al. (2006).

Figure 2 shows the distribution of the in-

Table 1—Continued

Name	ℓ (°)	$_{(^{\circ})}^{b}$	z	Scintillate?	x	$\theta_s$ (mas)	$\theta_i$ (mas)	N	$\chi^2$	$ heta_{ m NE2001} \  m (mas)$
J1327+2210	3.380	80.527	1.400	N	1	1.6	1.2	4	28	0.6
J1407 + 2827	41.862	73.251	0.076	N	1	0.0	5.0	8	9	0.5
J1642 + 6856	100.705	36.621	0.751	Y	1	1.2	1.7	13	46	0.8
J1656+6012	89.627	37.430	0.623	Y	0	6.8	0.3	3	0.1	0.8
J1746 + 6226	91.621	31.320	3.889	$Y_1$	0	2.7	0.2	5	19	0.8
J1812 + 5603	84.587	27.473		Y	0	3.3	0.3	3	12	0.8
J1823 + 6857	99.210	27.669		Y	1	1.8	1.6	4	12	0.9
J1927 + 6117	92.726	19.446	•••	$Y_1$	1	1.8	1.5	5	1	1.0
J2002+4725	82.219	8.793		$Y_1$	1	0.0	2.7	3	4	1.8
J2009+7229	105.355	20.180		Y	0	1.3	0.3	3	21	1.1
J2022+6136	96.082	13.775	0.227	N	0	3.1	0.4	15	30	1.4
J2230+6946	111.248	10.164		Y	0	2.4	0.3	7	16	2.0
J2311+4543	105.315	-13.703	1.447	Y	0	2.4	0.4	5	26	1.4
B0955+476	170.055	50.730	1.873	Y	1	2.1	0.1	7	34	1.0
B1130+009	264.364	57.582		N	0	1.8	0.9	4	51	0.9
B1226 + 373	147.142	78.938	1.515	N	1	2.8	0.1	4	15	0.5
B1236+077	294.112	70.170	0.400	N	1	1.4	0.3	3	48	0.8
B1402+044	343.669	61.169	3.211	N	1	2.2	0.3	6	48	0.6
B1432+200	21.387	65.299		$Y_1$		2.3	0.0	3		0.5
B1459 + 480	81.122	57.419		Y	0	1.6	1.1	4	110	0.8
B1502+036	2.226	50.254	0.413	$Y_1$		1.0	2.9	3	0.2	0.7
B1502 + 106	11.381	54.580	1.833	N	1	2.4	0.2	6	12	0.6

<sup>&</sup>lt;sup>a</sup>Both  $\nu^{-1}$  and  $\nu^{0}$  dependences for the intrinsic diameter produced equal  $\chi^{2}$ .

NOTE.—Sources are indicated to be either scintillators (Y), non-scintillators (N), or sources observed to vary once and presumed to be scintillators (Y<sub>1</sub>); x is the spectral index for the frequency dependence of the intrinsic diameter, equation (1);  $\theta_s$  and  $\theta_i$  are the inferred scattering and intrinsic diameters, respectively; N and  $\chi^2$  are the number of data and chi-square in the fit for equation (1); and  $\theta_{\text{NE}2001}$  is the predicted interstellar scattering diameter from the NE2001 model.

ferred scattering diameters plotted as a function of Galactic coordinates. We have considered the distribution of the sources on the sky as a function of both Galactic latitude b and ecliptic latitude  $\beta$  and the distribution as a function of solar elongation. There is no statistically significant correlation of the inferred scattering diameter with either coordinate (strictly, the absolute value of the coordinate), nor with  $\cos(|b|)$  or  $\cos(|\beta|)$ . (Typical correlation coefficients are approximately 0.1.) The use of the cosine of the angle  $[\cos(|b|)$  or  $\cos(|\beta|)]$  attempts to compensate for the increased amount of sky at low latitudes. There is also no correlation between inferred scattering diameter and solar elongation.

The lack of a correlation of the scattering diameter with Galactic latitude would appear to be at odds with previous determinations that interstellar scattering increases rapidly at low latitudes (e.g., Rao & Ananthakrishnan 1984). However, while no longitude selection criterion was applied in constructing our sample, our sample is nonetheless weighted strongly toward the outer Galaxy. We have no sources with longitudes in the range  $-60^{\circ} < \ell < 60^{\circ}$ , and only a few at low latitudes in the range  $-120^{\circ} < \ell < 120^{\circ}$ . Thus, we attribute the apparent lack of a correlation between scattering diameter and Galactic latitude as a result of having few, essentially no, lines of sight into the inner Galaxy.

While there is no correlation of scattering diameter with Galactic latitude for the entire set of sources, scintillating AGN are consistently at lower Galactic latitudes than the non-scintillating AGN. Table 2 shows that the average absolute values for the Galactic latitudes of scintillating and non-scintillating sources differ by nearly 20°. No such difference is found for the average (absolute) ecliptic latitude.

Figure 3 shows a histogram of the inferred scattering diameters. We have used a Kolmogorov-Smirnov test to assess whether scintillating AGN have a different distribution of inferred scattering diameters as compared to the non-scintillating AGN. We find no statistical difference: the scattering diameters of scintillating AGN do not differ appreciably from those of the non-scintillating AGN.

Examination of the scattering diameters inferred for individual objects indicates that some of

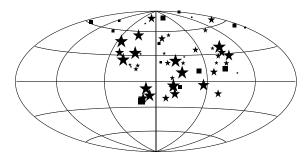


Fig. 2.— The distribution of sources observed as a function of Galactic coordinates. The Galactic anticenter is at the center of the plot, and longitude increases to the left. Stars indicate sources that scintillate; squares indicate non-scintillating sources. The size of the symbol is qualitatively proportional to the inferred scattering diameter.

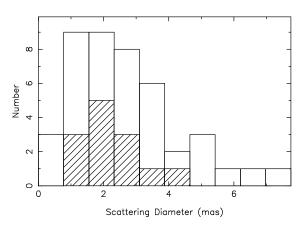


Fig. 3.— The histograms of scattering diameters. The open histogram shows the distribution for the scintillating sources; the hatched histogram shows the distribution for the non-scintillating sources.

TABLE 2 STATISTICAL MEASURES

	Scintillators	Non-scintillators			
mean		de (absolute value) $46^{\circ}.3 \pm 7^{\circ}.0$			
mean	ecliptic latitude (absolute value) $34^{\circ}.9 \pm 4^{\circ}.3$ $28^{\circ}.8 \pm 4^{\circ}.9$				
mean (mas) median (mas)	Scattering Dia $2.1 \pm 0.2$ $1.9$	ameters (at 1 GHz) $2.1 \pm 0.2$ $2.0$			
mean (mas) median (mas)	Redshifts $1.38 \pm 0.18$ $1.29 \pm 0.31$ $1.27$ $1.40$				

the largest scattering diameters result from AGN for which no measurements exist below 1 GHz. In order that these not bias our result, we removed these and repeated the K-S test analysis. There is no change in the result, that the scattering diameters for the scintillating and non-scintillating AGN are consistent with having been drawn from the same distribution. Both the mean and the median scattering diameter for scintillating and non-scintillating sources is approximately 2 mas (Table 2).

From the entire sample, 37 AGN (64%) have measured redshifts. There appears to be little difference in the redshift distribution of the scintillating and non-scintillating AGN, with the two populations having similar means and medians (Table 2). Figure 4 shows the distribution of the scattering diameters as a function of redshift. We have determined the correlation between the scattering diameters and redshifts for the entire sample, as well as splitting it into the two populations, scintillating and non-scintillating. There is no correlation of the scattering diameter with redshift for the entire sample. There may be a marginal correlation, at the 5% confidence level, between the scattering diameters and redshift, in the opposite sense for the scintillating and nonscintillating sources. That is, the scattering diameters of scintillating (non-scintillating) AGN may

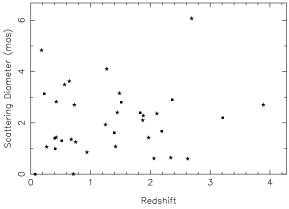


Fig. 4.— The distribution of scattering diameters as a function of redshift. Stars indicate sources that scintillate; squares indicate non-scintillating sources.

become smaller (larger) at higher redshifts.

#### 4. Discussion and Conclusions

In one sense, our results are broadly consistent with what is known about intraday variability and interstellar scattering. In our sample, scintillating AGN lie typically at lower Galactic latitudes, consistent with the notion that the scintillation responsible for IDV results from the Galactic ISM ( $\S1$ ).

In addition to the ISM, other ionized media along the lines of sight to these sources are the interplanetary medium (IPM) and the intergalactic medium (IGM). It is possible that the IPM could contribute angular broadening at a level sufficient to be detectable in this analysis, particularly given the use of 0.33 and 0.61 GHz observations. The lack of a correlation with either the ecliptic latitude (Table 2) or solar elongation, however, implies that the IPM makes no detectable contribution in these observations. The lack of a strong correlation with redshift and the systematically lower Galactic latitude of the broadened sources suggests that the IGM makes no detectable contribution to our observations, either.

In a further effort to differentiate the Galactic contribution of scattering from any possible intergalactic contribution, we have searched for pulsars within 1° of the AGN in our sample. We find no pulsars this close to any of our sources. Given the relatively low density of pulsars on the sky, a significantly larger sample of AGN would be required in order to make such a comparison.

On the face of it, the result that scintillating AGN are broadened at levels comparable to those of the non-scintillating AGN appears to contradict the requirement (§1) that in order to display scintillation, a source must be sufficiently compact. One possibility is that scattering is, in fact, not important at all and that we have mistakenly attributed the effects of intrinsic structure to angular broadening. We regard this as unlikely, given that the angular diameters of the sample of sources, as a whole, scale approximately as expected from interstellar scattering.

In fact, the magnitude of the estimated broadening does not appear to be problematic from the standpoint of quenching the scintillations. Taking 2 mas at 1 GHz as a characteristic scattering diameter (Table 2), the implied scattering diameter at 5 GHz is 80  $\mu$ as, comparable to the value derived for a number of the well-known scintillating sources (e.g., Rickett et al. 1995; Rickett, Kedziora-Chudczer, & Jauncey 2002; Dennett-Thoppep&cdeeBough components are then observed 2003; Bignall et al. 2003).

A notable feature of the most extreme IDV sources is that detailed analyses of their light curves suggest that the scattering medium responsible for the scintillation lies quite close to the Sun  $(\approx 25 \text{ pc})$ . If local material was responsible for

the scintillation of all scintillating AGN, we would not expect a difference between the average Galactic latitude of scintillating and non-scintillating sources (Table 2). That such a difference exists suggests that the scintillation for most scintillating AGN results from scattering material associated with the Galactic ISM.

A consistent explanation for these results is obtained if the scintillation is produced from small "clumps" of scattering material, distributed throughout the Galactic disk. For instance, Dennett-Thorpe & de Bruyn (2003) determine that a "thin screen" is responsible for the extreme IDV of J1819+3845, with the screen being about 10 pc distant and having an internal level of scattering measured by  $C_n^2 = 0.5 \text{ m}^{-20/3}$ . They do not provide a quantitative estimate of the thickness of this screen, but, in order that the screen be "thin," it must surely be the case that its thickness is  $\Delta L \lesssim 1$  pc.

Suppose we require that the scattering contributed by such a clump not make a significant contribution to the angular broadening. For illustration purposes, we adopt the amount of broadening contributed by the clump to be  $\theta_{s,cl} \sim 0.2$  mas, which would be only a 10% contribution to the typical broadening diameter that we measure. The resulting scattering measure SM (Cordes & Lazio 2006) is then SM<sub>cl</sub>  $\sim 10^{-4.8}$  kpc m<sup>-20/3</sup>. If the clump has  $C_n^2=0.5$  m<sup>-20/3</sup>, the implied thickness is 0.05 pc ( $\sim 10^4 \text{ AU}$ ), which would certainly qualify as "thin." Moreover, following Rickett et al. (1995) and Rickett (2002), it can be shown that a more distant scattering clump tends to produce a lower scintillation index.

Thus, our picture is one in which the Galactic disk contains (small) "clumps" of scattering material. Lines of sight through the disk are scattered by the broadly distributed ionized interstellar medium, so that AGN over the range of latitudes that we observe have measurable scattering diameters. Some (many?) lines of sight pass through one of these clumps, and AGN having to scintillate. However, the clumps are small enough that they produce effectively no additional broadening. This scenario is also broadly consistent with the notion of "clumps" of material producing extreme scattering events (Fiedler et al. 1987) and parabolic arcs in pulsar dynamic spectra (Hill et al. 2005).

We can also use the difference between the scintillating and non-scintillating sources to set quantitative limits on the amount of radio-wave scattering contributed by the IGM. We adopt 0.5 mas at 1 GHz ( $\approx 3\sigma$  from Table 2) as the upper limit on the difference in the amount of scattering between the two populations. The implied scattering measure is SM  $\lesssim 10^{-4}$  kpc m<sup>-20/3</sup> (Cordes & Lazio 2006). In turn, the scattering measure is given by

$$SM = C_{SM} \overline{F n_e^2} D, \qquad (2)$$

where D is the distance, F is a fluctuation parameter encapsulating aspects of the microphysics of the plasma,  $n_e$  is the electron density, and  $C_{\rm SM}=1.8~{\rm m}^{-20/3}~{\rm cm}^6$  is a constant. For a characteristic redshift of approximately unity (Figure 4), the equivalent (angular-size) distance is  $D\approx 1.5~{\rm Gpc}$ , implying  $\overline{F}n_e^2\lesssim 10^{-10.5}~{\rm cm}^{-6}$ .

For a baryonic matter density  $\Omega_b h^2 = 0.127$  (Spergel et al. 2006), the intergalactic electron density can be no larger than  $\overline{n_e} < 2.2 \times 10^{-7}$  cm<sup>-3</sup>, assuming that helium is fully ionized (Sokasian, Abel, & Hernquist 2002). Thus, we require  $F \lesssim 10^3$ , so as not to violate the inferred limits on scattering. For reference, in the diffuse Galactic ISM,  $F \approx 0.2$ , and in the Galactic spiral arms,  $F \sim 10$ . In turn, the F parameter is

$$F = \zeta \epsilon^2 \eta^{-1} \ell_0^{-2/3}, \tag{3}$$

where  $\zeta$  is the normalized second moment of the fluctuations,  $\epsilon$  is the fractional variance in  $n_e$  within the plasma,  $\eta$  is the filling factor, and  $\ell_0$  is the largest scale on which the density fluctuations occur (or outer scale, if the plasma is turbulent), in parsec units. Assuming that  $\zeta \sim \epsilon \sim 1$ , we conclude that  $\eta \ell_0^{2/3} \gtrsim 10^{-3}$ .

The IGM is thought to be permeated by shocks (Davé et al. 2001), which might be expected to drive  $\eta \to 1$ . Given the larger scales available in the IGM,  $\ell_0 \sim 1$  Mpc would not be unreasonable. We are forced to conclude that the current limits on intergalactic scattering, while broadly consistent with the current picture of the IGM, do not yet place significant constraints on its properties.

While we find no indications of intergalactic scattering, future observations are warranted. In particular, if a scintillating AGN is found close to the line of sight to a pulsar, a comparison between the two lines of sight would provide strong constraints on the amount of Galactic vs. intergalactic scattering. Also, higher-sensitivity observations (e.g., with the very long baseline High Sensitivity Array or HSA) targeting scintillating AGN with larger diameters may provide additional constraints. Many of the AGN with the largest diameters are not detected at the lower frequencies, frequencies at which the VLBA alone has a relatively low sensitivity. The HSA could be used to verify whether these AGN do indeed have such large scattering diameters or assess to what extent intrinsic structure contaminates the scattering diameter estimates.

We summarize our findings as follows. In our sample of 58 AGN, approximately 75\% of the sample exhibit intraday variability (interstellar scintillation) with the other 25% not showing intraday variability. Interstellar scattering is measurable for most of these AGN, and the typical broadening diameter is 2 mas. Scintillating AGN are typically at lower Galactic latitudes than the nonscintillating AGN, consistent with the scenario that intraday variability is a propagation effect from the Galactic interstellar medium. The magnitude of the inferred interstellar broadening measured toward the scintillating AGN, when scaled to higher frequencies, is comparable to that determined from analyses of the light curves for the more well-known intraday variable sources. However, we find no difference in the amount of scattering measured toward the scintillating versus non-scintillating AGN. A consistent picture is one in which the scintillation results from localized regions ("clumps") distributed throughout the Galactic disk, but which individually make little contribution to the angular broadening. In our sample, 63% of the AGN have measured redshifts. At best, a marginal trend is found for scintillating (non-scintillating) AGN to have smaller (larger) angular diameters at higher redshifts. Finally, while broadly consistent with the scenario of a highly turbulent intergalactic medium, our observations do not place significant constraints on its properties.

We thank the referee for suggestions that improved the presentation of these results. The National Radio Astronomy Observatory is a fa-

cility of the National Science Foundation operated under cooperative agreement by Associated Universities, Inc. This research has made use of the United States Naval Observatory (USNO) Radio Reference Frame Image Database (RRFID); NASA's Astrophysics Data System bibliographic services; the SIMBAD database, operated at CDS, Strasbourg, France; and the NASA/IPAC Extragalactic Database (NED) which is operated by the Jet Propulsion Laboratory, California Institute of Technology, under contract with the National Aeronautics and Space Administration. Basic research in radio astronomy at the NRL is supported by the NRL Base funding.

#### REFERENCES

- Bignall, H. E., Macquart, J.-P., Jauncey, D. L., Lovell, J. E. J., Tzioumis, A. K., & Kedziora-Chudczer, L., 2006, ApJ, in press
- Bignall, H. E., Jauncey, D. L., Lovell, J. E. J., Tzioumis, A. K., Kedziora-Chudczer, L., Macquart, J.-P., Tingay, S. J., Rayner, D. P., & Clay, R. W. 2003, ApJ, 585, 653
- Cordes, J. M., & Lazio, T. J. W. 2006, ApJ, submitted; astro-ph/0207156
- Davé, R., et al. 2001, ApJ, 552, 473
- Dennett-Thorpe, J., & de Bruyn, A. G. 2003, A&A, 404, 113
- Dennett-Thorpe, J., & de Bruyn, A. G. 2002, Nature, 415, 57
- Fey, A. L. & Charlot, P. 1997, ApJS, 111, 95
- Fiedler, R. L., Dennison, B., Johnston, K. J., & Hewish, A. 1987, Nature, 326, 675
- Heeschen, D. S. 1984, AJ, 89, 1111
- Hill, A. S., Stinebring, D. R., Asplund, C. T., Berwick, D. E., Everett, W. B., & Hinkel, N. R. 2005, ApJ, 619, L171
- Jauncey, D. L., Bignall, H. E., Lovell, J. E. J., Kedziora-Chudczer, L., Tzioumis, A. K., Macquart, J.-P., & Rickett, B. J. 2000, in Astrophysical Phenomena Revealed by Space VLBI, eds. H. Hirabayashi, P. G. Edwards, & D. W. Murphy (ISAS) p. 147

- Jauncey, D. L., & Macquart, J.-P. 2001, A&A, 370, L9
- Jauncey, D. L., Johnston, H. M., Bignall, H. E., Lovell, J. E. J., Kedziora-Chudczer, L., Tzioumis, A. K., & Macquart, J.-P. 2003, Ap&SS, 288, 63
- Jauncey, D. L., Lovell, J. E. J., Koyama, Y., & Kondo, T. 2006, AJ, Submitted
- Johnston, K. J., et al. 1995, AJ, 110, 880
- Lovell, J., Jauncey, D., Senkbeil, C., Shabala, S., Bignall, H., Macquart, J.-P., Rickett, B., & Kedziora-Chudczer, L. 2007, in Small Ionized and Neutral Structures in the Diffuse Interstellar Medium, eds. M. Haverkorn & W. M. Goss (ASP: San Francisco) in press
- Lovell, J. E. J., Jauncey, D. L., Bignall, H. E., Kedziora-Chudczer, L., Macquart, J.-P., Rickett, B. J., & Tzioumis, A. K. 2003, AJ, 126, 1699
- Ma, C., Arias, E. F., Eubanks, T. M., et al. 1998, AJ, 116, 516
- Ojha, R., Fey, A. L., Lazio, T. J. W., Jauncey, D., Lovell, J., & Kedziora-Chudczer, L. 2006, ApJS, 166, 37 (Ojha et al. 2006)
- Ojha, R., Fey, A., Jauncey, D. L., Lovell, J. E. J., & Johnston, K. J. 2004, ApJ, 614, 607
- Quirrenbach, A., Witzel, A., Kirchbaum, T. P., Hummel, C. A., Wegner, R., Schalinski, C. J., Ott, M., Alberdi, A., & Rioja, M. 1992, A&A, 258, 279
- Rao, A. P., & Ananthakrishnan, S. 1984, Nature,  $312,\,707$
- Rickett, B. J., Kedziora-Chudczer, L., & Jauncey, D. L. 2002, ApJ, 581, 103
- Rickett, B. J., Witzel, A., Kraus, A., Krichbaum, T. P., & Qian, S. J. 2001, ApJ, 550, L11
- Rickett, B. J., Quirrenbach, A., Wegner, R., Krichbaum, T. P., & Witzel, A. 1995, A&A, 293, 479
- Rickett, B. J. 2002, Publ. Astron. Soc. Aust., 19,  $100\,$

Rickett, B. J. 1990, ARA&A, 28, 561

Sokasian, A., Abel, T., & Hernquist, L. 2002, MN-RAS, 332, 601

Spergel, D. N., et al. 2006, ApJ, submitted; astro-ph/0603449

Walker, M. A. 1998, MNRAS, 294, 307

This 2-column preprint was prepared with the AAS IATEX macros v5.2.